

DISPLAY DESIGN CONCEPTS FOR PHYSICS BASED STIMULATION OF NIGHT VISION GOGGLES¹

Jeff Clark, Brad Colbert & Kris Pribadi,
Program Manager, Senior Systems Analyst, Senior Systems Engineer,
Renaissance Sciences Corporation

&

Joe Riegler
Human Factors Engineer
The Boeing Company

&

Gretchen Anderson
Human Factors Engineer
L-3 Communications, Link Simulation and Training

Abstract

The physical challenges associated with sensor-in-the-loop Night Vision Goggle (NVG) training systems are well documented. Depth-of-focus sensitivity and the need for light-tight environments and NVG-compatible cockpit modifications, as examples, can be overcome, with some tradeoffs, by appropriate system design. The challenge of producing realistic NVG representations, however, continues to yield unpredictable results, particularly when there is an attempt to produce simultaneous NVG-aided and unaided representations. Systems integrators often engage in an iterative cycle of display tuning in an attempt to accommodate subjective accuracy assessments from engineers and customers who provide differing feedback. It is assumed that iterative tuning increases the overall accuracy of the system, when in fact it most often simply trades one type of error for another. Research at the Air Force Research Laboratory, Warfighter Readiness Research Division, Mesa, AZ, investigated the application of previously developed physics-based NVG simulation techniques as a foundation for a deterministic approach to sensor-in-the-loop NVG stimulation. Key research objectives included the quantification of display radiation, the implementation of a physics-based NVG stimulation capability, and the quantification of error in NVG stimulation scenes. Key performance metrics including NVG-aided scene luminance accuracy, unaided scene luminance accuracy, and unaided scene color accuracy were captured for varying test cases and analyzed. The relationship between these metrics was found to be inherent to the spectral characteristics of a display's output and is, in fact, fixed for a given display system configuration. These tradeoffs are not widely understood by users of display systems, and while many display professionals intuitively understand the application impact of these tradeoffs, there is insight to be gained by quantifying the exact nature of these challenges. Selective filtering of specific wavelengths of the display output in conjunction with the employment of physics-based rendering techniques was shown to produce a more favorable and predetermined compromise between NVG realism and out-the-window realism. Indeed, it was found that with the help of certain light measurements devices and physics-based techniques, these tradeoffs can be understood and minimized during system design rather than explored later through trial and error. Finally, lessons learned yielded display design insights which are summarized for the consideration of display manufacturers.

Background

In considering the characteristics of a display system intended for replicating the human experience of using NVGs in the night environment, it is appropriate to first quantify the night environment as seen by NVGs *and* by the human eye. For the purposes of numerical analysis a common light measurement geometry was chosen: flux density per solid viewing angle. **Luminance** and **Radiance** were used to quantify natural and simulated flux density (W/cm^2) per solid viewing angle (sr) in $\text{W}/\text{cm}^2/\text{sr}$ per nanometer. These quantities may be measured at a single wavelength or integrated over a specified domain of wavelengths. By varying the wavelength ranges over which radiance values are integrated, the light quantities relevant to the sensors of interest, namely NVGs and the human eye, are captured. Three integrations of light quantities were prominent in the study:

Night Vision Imaging System (NVIS) Radiance in $\text{W}/\text{cm}^2/\text{sr}$ describes a quantity of NVG-sensitive light. In this case, radiance is integrated over the NVG-sensitive wavelengths and convolved with the response filter of the NVG sensor itself. In training systems applications, there are several response filters that might apply. The Class B minus blue filter typical to aviator goggles employed in non-heads up display (HUD) equipped aircraft is used for all analyses that follow. The NVIS Radiance, Class B quantity is abbreviated as NR_B . See the NR_B response filter in Fig. 1.

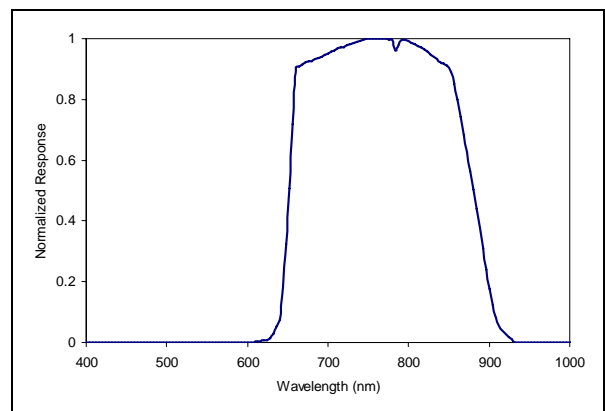


Fig. 1: NVG Class B response

Luminance is the visible counterpart of the more generalized measure of radiance. It is quantified with a variety of units that typically carry a historic observation-based meaning. Foot-lamberts (**FL**) was the unit chosen for all numerical analyses as this is the unit used by the light measurement equipment used in the research.

Visible Radiance is a measure which was used to help relate NVIS radiance and luminance in the research. It carries the unit of $W/cm^2/sr$ and will describe a quantity of human-sensitive light. As such, it is the radiance integrated over the visible wavelengths, and it is also convolved with the response filter of the human eye. In this context, there are several response filters that might apply: those consistent with **photopic**, **mesopic**, and **scotopic** vision states. For simplicity, the analysis will assume photopic vision response only, although a caveat is warranted here in that it may sometimes be possible for NVG viewing applications to produce mesopic viewing conditions in starlight conditions. See the photopic human vision response filter in Fig. 2. Visible radiance ($W/cm^2/sr$) and luminance (FL) are related by this conversion factor: Luminance = visible radiance / $5.016E-7$.

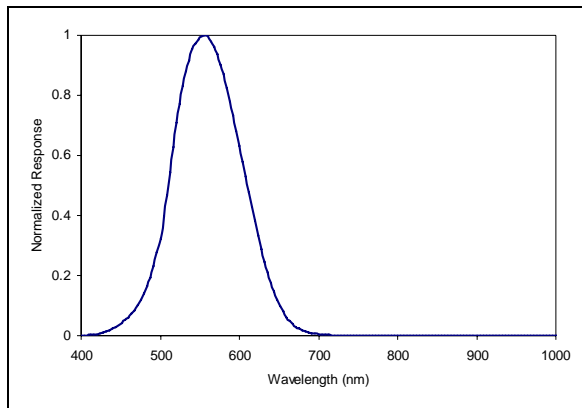


Fig. 2: Photopic response

Physical Properties of Night Sky Radiation

The quantification of night sky radiation is the first step in approaching the challenges of physics-based NVG stimulation. This list summarizes the most meaningful components of night sky radiation (Jensen, 2001; Leinert, 1998): 1) **The Moon**. When present, moonlight is the dominant source of illumination in the night scene; 2) **Zodiacal Light**. Sunlight is reflected toward Earth by small particles present in the solar system; 3) **Starlight**. Integrated light from the visible star sphere and the planets lights the night scene; 4) **Airglow**. Photochemical luminescence in the atmosphere produces light emission in the visible and near infrared wavelengths; and 5) **Diffuse Galactic and Cosmic Light**. Also known as Cirrus, light originating outside our galaxy produces a measurable component of the night sky radiation on Earth. A quantification of the contribution of the Sun during periods of astronomical twilight before sunrise and after sunset is not included here. This source of illumination dominates all others when present.

Night Sky Radiation under Clear Starlight Conditions. In the absence of moonlight, the numerous but faint contributors summarized above constrain the magnitude and the spectral makeup of the light that illuminates everything in the night scene. Fig. 3 shows the typical radiance, by wavelength, observed for each of the night sky radiation contributors. Note

that contribution in the near infrared wavelengths tends to be meaningfully greater than that in the visible wavelengths.

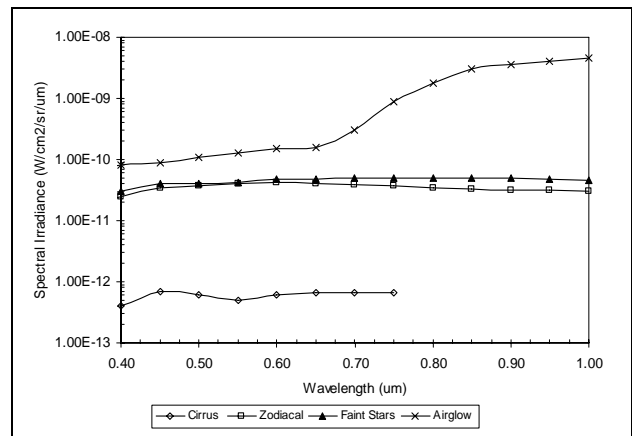


Fig. 3: Clear starlight spectral radiance

Night Sky Radiation under Lunar Illumination Conditions. Under lunar illumination conditions, the moonlight present in the night sky is the primary modeling concern as all other sources are “in the noise” compared to the lunar component. Clearly, the magnitude of the lunar contribution is much higher in whole, but one should also consider the spectral makeup of the lunar contribution. In this case, energy radiated by the sun is reflected by the Moon before entering our atmosphere. One can approximate the relative response of lunar illumination by convolving the lunar reflectance (Lawrence, 2003) (Fig. 4) with the solar spectral irradiation data (Moon, 1940), and the spectral transmission of Earth atmosphere (Moon, 1940) to produce the relative response curve found in Fig. 5.

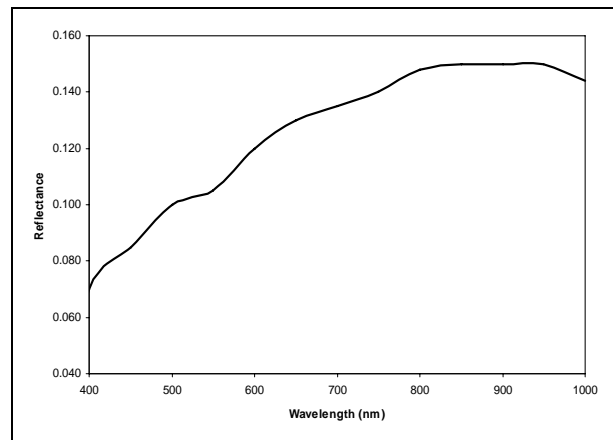


Fig. 4: Absolute lunar spectral reflectance

Using this approximation, the spectral makeup of the lunar irradiation does appear to be meaningfully different from that of starlight conditions.

Simulating Night Sky Radiation

Now, with the relative responses of the human eye, NVG, lunar illumination, and starlight illumination all defined, the spectral response of the key components of the physics-based NVG stimulation application can be summarized. Fig. 5 plots all of these response/sensitivity curves on the same axes.

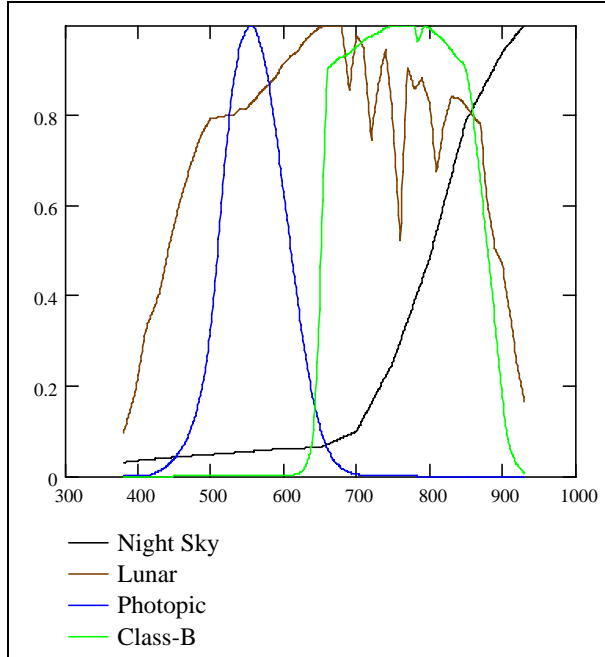


Fig. 5: Key components spectral response

By integrating radiance over the wavelength domains of interest and by converting to luminance as applicable, the physical properties of the night sky radiation can be consolidated into scalar light measurement quantities that may be used as simulation coefficients in real time applications, measured in the simulation laboratory, and confirmed in the real world using available instruments. For example, the derived values for “brightness” to the human eye and to NVG are shown in Table 1 below.

Table 1: Integrations of night sky radiance

Component	Visible Luminance (FL)	Visible Radiance (W/cm ² /sr)	NVIS Radiance (W/cm ² /sr)
Airglow	2.9E-5	1.4E-11	3.2E-10
Zodiacal Light	8.5E-6	4.3E-12	8.2E-12
Integrated Starlight	9.3E-6	4.7E-12	1.1E-11
Cirrus	1.2E-7	6.0E-14	7.9E-14
Total	4.6E-5	2.3E-11	3.4E-10

For modeling lunar illumination scenarios, the values found in Table 2 are typical visible and NVIS flux densities.

Table 2: Integration of lunar radiance

Moon Phase (90 degree elevation angle)	Visible Luminance (FL)	Visible Radiance (W/cm ² /sr)	NVIS Radiance (W/cm ² /sr)
100% disc	3.45E-2*	1.7E-8	1.2E-8

*(Biberman, 2000)

The visible radiance figure found in Table 2 is a simple conversion of the luminance figure. The NVIS radiance figure of 1.2E-8 is a derived estimation produced by applying the integrated lunar response curve found in Fig. 5 to an integration of Planck black body radiation, taking into account the

surface area of the moon and the mean distances of Earth, Moon, and Sun (Jensen, 2001). This estimation is consistent with field measurements recorded at AFRL/HEA.

It is useful to go a step further in describing the nature of the visible light by separately integrating the combined visible light under starlight and lunar conditions over the blue, green, and red wavelengths separately as shown in Table 3. These values provide an approximation of the natural color balance present in the night sky. Blue radiance is derived by integrating visible radiance from 400-500 nm; green and red values are integrated over 500-600 nm and 600-700 nm, respectively.

Table 3: Radiance integrations of night sky colors

Illumination Source	Blue Radiance (W/cm ² /sr)	Green Radiance (W/cm ² /sr)	Red Radiance (W/cm ² /sr)	NVIS Radiance (W/cm ² /sr)
Clear Starlight	1.3E-12	1.7E-11	4.6E-12	3.4E-10
100% lunar disc	1.0E-9	1.3E-8	3.4E-9	1.2E-8

Converting the visible values from Table 3 above to luminance, Table 4 represents these quantities in units familiar to light measurement instruments and display system analysis.

Table 4: Luminance contributions of night sky colors

Illumination Source	Blue Luminance (FL)	Green Luminance (FL)	Red Luminance (FL)
Clear Starlight	2.6E-6	3.5E-5	9.2E-6
100% lunar disc	2.0E-3	2.6E-2	6.8E-3

Simulating Night Scene Radiance. The night sky radiation is the dominant factor in predicting the quantities of light and spectral weighting of light in any given night scene in general, and it is therefore of particular importance here. Techniques for producing complex, *parametric* models of the atmosphere and describing the reflection of light in the environment are well documented (Berk, 1989; Biberman, 2000; Jensen, 2001; Leinert, 1998). For example, illumination of scene content by man-made lighting will have different physical properties than that described above. Also, while many naturally occurring materials have similar reflectance characteristics in the visible and near infrared domain, there are many materials that do not. It should be assumed that sophisticated physics-based modeling of the night environment is a critical component to any application producing a physics-based stimulation of NVGs. Rather than discussing the intermediate modeling required, the analyses here will focus on the final result of such a physics-based simulation, the differing quantities of light, visible and near infrared, assigned to nearby surfaces in a scene, creating a relative contrast that ultimately impacts the visual performance, aided and unaided, of the viewer.

Display Representation of Simulated Night Sky Radiation. In order to “close the loop” in a physics-based stimulation application, the output of the display must be accurately modeled as a function of its full domain of inputs and in a common computational and units space. In the initial phases of the research, display exemplars were measured in the laboratory and in the field in an effort to quantify their perform-

ance with the same light measurement approach as is described above. The displays encountered were driven by a similar class of Barco CRT-based projectors, although they were integrated in a broad range of display geometries and with a broad range in projector age. It was generally found that spectral makeup of the projected light was very similar or identical, likely due to the fact that like phosphors are utilized by many CRT projector systems. As an example, the spectral distributions of a Barco 908 Projector are plotted in Fig. 6 and Fig. 7.

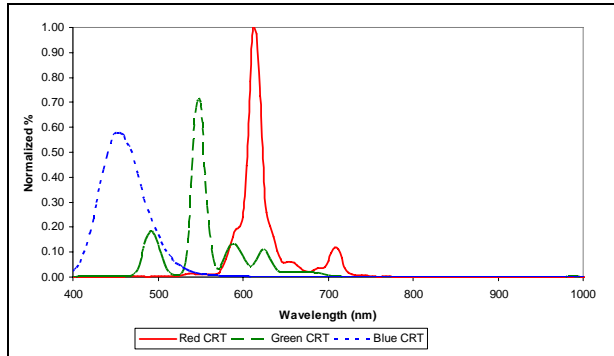


Fig. 6: CRT spectral intensity example (Barco 908)

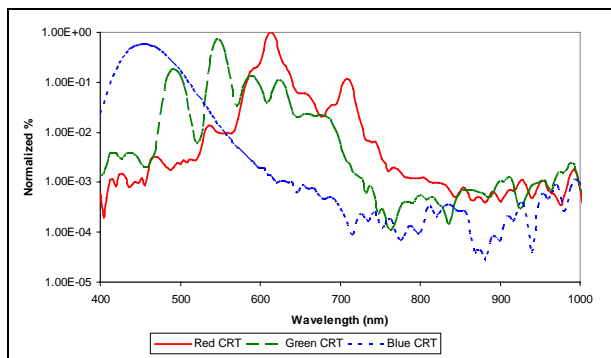


Fig. 7: Logarithmic CRT spectral intensity example (Barco 908)

Note that while there are trace amounts of near infrared energy present in each display channel, the significant NVIS response is produced in the red wavelengths. Therefore, it will not be possible to achieve a natural color balance between blue, green, red, and near infrared. While the spectral profile was consistent among the displays tested, the profile of light magnitudes varied significantly with display projection geometry. The magnitude in the near infrared wavelengths generally followed a similar profile. As an example, Figs. 8 and 9 show luminance and NR_B as a function of input pixel value measured from a Barco 801 RetroGraphics display system. Other systems encountered in the study produced less than a tenth of the output of this display. Differences in dynamic range performance required differing approaches to best utilize the dynamic range (visible and NVIS) and the precision (number of intensities) available to the simulation. Approaches used to optimize these metrics are captured in the case studies that follow.

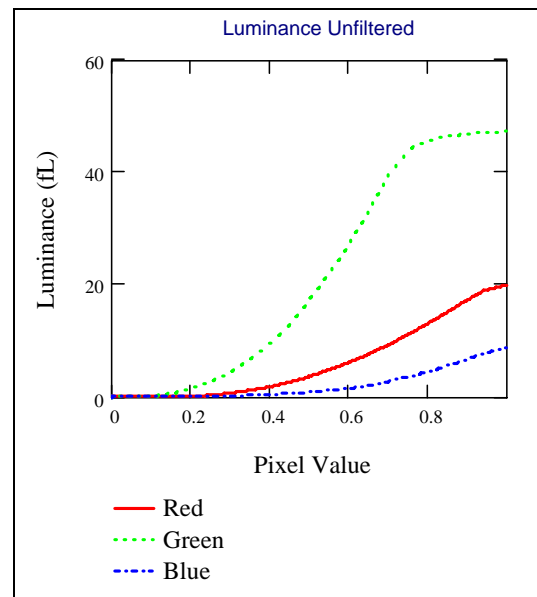


Fig. 8: CRT luminance characterization example

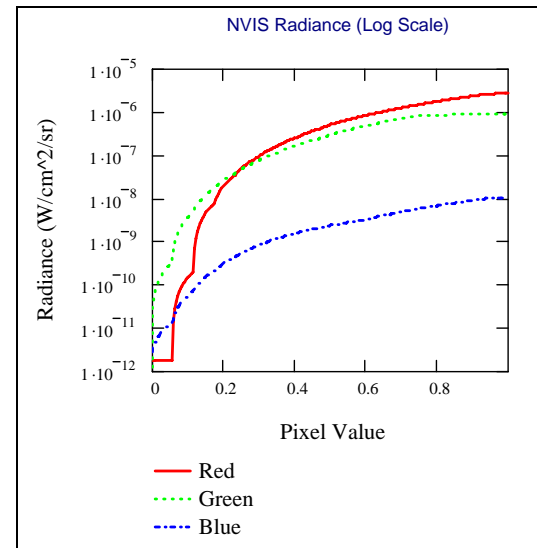


Fig. 9: CRT NVIS radiance characterization example

Test Cases

The test cases summarized below offer two relative extremes of CRT display brightness and the application of physics-based stimulation to both. While the test cases demonstrate that a high level of accuracy can be achieved for the sensor-in-the-loop scene, they also illustrate the tradeoff between NVG output accuracy and unaided-OTW luminance accuracy in the stimulation application. For the purposes of the research, this tradeoff was approached aggressively in favor of NVG accuracy as a priority over unaided luminance accuracy. In each case, the accuracy of the NR_B representation was maximized, giving it the highest priority as engineering decisions were made within the constraints of a given visual system configuration. From this point, effort was made to maximize the unaided accuracy by subjective assessment without affecting the NR_B characteristics of the configuration. So, while the NR_B

representation received a physics-based rendering treatment, the unaided representation did not. The case studies that follow will describe the approaches taken in the research to modulate the projected light in order to minimize the error in color balance, but especially error in NR_B and integrated luminance. While the impact of these tradeoffs was mitigated significantly over traditional approaches, the NVIS radiation contribution could not be established accurately without impacting luminance accuracy in *some* measure (red luminance in particular).

While the dynamic range capabilities (in luminance and NR_B) are inherent to a display in a particular configuration and cannot be increased, one does have control over the way in which images are composed with the three color channels of the projector. It was found then, that one does have the ability to influence accuracy tradeoffs according to relative tolerance for errors in NR_B , integrated luminance, and color balance. More aggressive projector settings (brightness, contrast, etc.) are possible if spectral filtering techniques are engineered to allow it. These more aggressive projector settings, in turn, provided a higher dynamic range capability to the NVG stimulation than would have otherwise been possible.

The subjective assessment of unaided OTW light levels was focused on lowering total integrated luminance as a higher priority than maintaining a natural color balance. Traditional NVG stimulation systems often have the unfortunate characteristic of unaided OTW levels exaggerated to the point that the terrain can be easily resolved without using the NVGs. Avoiding this potential negative training artifact was a specific priority in the approach. The visual spectrum simulation data appearing here in the Background was not compiled and derived until more recently and was, therefore, not available at the time the test cases were implemented. Current research and development efforts at AFRL/HEA include the development of combined rendering mathematics for the NVIS *and* visible spectra, but these techniques are not covered here.

The impact, in application, of unrealistic luminance representations of scene content is rarely *quantified* in simulator applications. To provide a measure of the impact of errors in light level in application context, the numerical analysis of the test cases was used to measure the error produced when rendering test patches of four intended albedos on the subject system. *Actual* contrast levels versus *intended* contrast levels are then calculated and, in the case of NVG output, related to a change in visual acuity under the viewing condition. The calculated difference in visual acuity (favorable or unfavorable) introduced by the visual system is offered as a very general metric from which application impact could be assessed on a case by case basis.

All test cases documented here utilized CRT-based projector technologies. Current development at AFRL/HEA also includes the application of these techniques to digital projector products, but that research is not covered here.

Research Tools Utilized for Test Cases

A collection of instruments, applications, and data was utilized to complete the research summarized by the test cases found in the next section: 1) **Photometers**. Instruments of varying sensitivity were used to measure luminance response of displays in bright and low-light scenarios. Full profiles of display response versus pixel value were stored for application ingestion; 2) **Radiometer**. This specialized instrument meas-

ures NR_B at high precision in low-light. Full profiles of display response versus pixel value were stored for application ingestion; 3) **SensorHost Software Model**. This AFRL/HEA-provided software provided data driven models for naturally-occurring NR_B levels. The software also provided a software model of the NVG sensor itself which was used to model NVG artifacts for injection into the stimulated scene. (i.e., halos); 4) **Rendering Test Application**. A software application that interfaced with SensorHost and ingested the stored display characterizations was used to render physics-based NVG stimulation scenes targeted for a specific display; and 5) **Field Data**. Measurements were collected from real-world night scenarios using the same instruments described above. This data provided a useful tool for confirmation of laboratory results.

Numerical Analysis Utilized in Test Cases

The numerical analyses that follow quantify the accuracy of the synthetic scenes by measuring light quantities viewed on the displays. This accuracy is tested with and without the use of the NVG, as both views are utilized for NVG missions. Accuracy metrics are captured under simulated clear starlight conditions and simulated full moon conditions. In each case, a series of four simulated diffuse reflective test patches are used to sample scene **luminance** accuracy. Representations of the four patches, having reflectivity values of 10%, 15%, 25%, and 90% are displayed and the resulting display luminance response is measured for each case and compared to the high precision software simulation ground truth that was intended. Comparison of the *intended* luminance values for each patch compared to the *actual* luminance values measured off of the display provides a snapshot of the unaided luminance accuracy of the configuration. The same four measurements are also taken with a calibrated NVG in the loop. In this case, a photometer was mated with the output of an NVG device that is simultaneously viewing one of the same four test patch values described above. Comparison of the *intended* NVG luminance values for each patch with the *actual* NVG luminance values measured off of the NVG provides a snapshot of the aided luminance accuracy of the configuration. NVG luminance is a derived value produced from high precision calibration data associated with the NVG used in the study. Intended and actual NVG luminance values are predicted using *intended* NR_B values (from the scene simulation ground truth) and *actual* NR_B values (measured off of the display using a radiometer). This approach has the advantage of holding constant certain time dependent variables that effect NVG performance (such as battery state). While the comparison of intended luminance versus actual luminance captures that native accuracy of the configuration in its simplest form, these values are difficult to relate to an impact to human viewing. Therefore, additional derived values are produced in each case.

First, the four test patches are paired in three combinations to produce three levels of simulated **contrast**, a key measure effecting visual acuity. There are a number of methods for measuring scene contrast. For the purposes of the analysis, the measure of *modulation contrast* was utilized, as defined in Eq. 1.

$$Contrast = \frac{Lum_{max} - Lum_{min}}{Lum_{max} + Lum_{min}} \quad (Eq.1)$$

General Observations

As with luminance, intended and actual contrast values are evaluated both for aided viewing (NVG) and for direct viewing of the out-the-window display (OTW). Contrast changes were evaluated for both aided and unaided representations, because of the desire to produce simulations that result in realistic simultaneous viewing conditions *both* aided and unaided (Martin, 2000). Contrast accuracy was evaluated at high, medium, and low contrast levels; 80%, 43%, and 20%, respectively.

Second, by making reasonable assumptions with respect to average reflectivity levels present in a scene, the average **scene luminance** was approximated and compared to the intended scene luminance (for the same set of assumptions) in the simulated ground truth.

Finally, with an understanding of the contrast and luminance deviation created by the entire system (display, image generator, rendering technique, and so forth), the accuracy of the NVG aided representation was quantified by comparing the visual acuity possible in the simulated scene to the visual acuity supported by the measured display, taking into consideration the errors in NR_B output. The effect of NVG scene luminance and target contrast on F4949G NVG-aided visual acuity (VA) is represented in Fig. 10, (unpublished AFRL/HEA laboratory data, 2005). Using this model, the change in maximum achievable visual acuity was approximated. While it is typically the case that studies involving displays would seek to maximize visual acuity, the goal here was to *preserve* the visual acuity characteristics of the simulated ground truth so that the *training system* experience of using NVGs might be representative of the *real-world* experience of using NVGs. Therefore, meaningful enhancement of visual acuity was to be specifically avoided as was degradation of visual acuity. It is evident from inspection of Fig. 10 that NVG-aided VA declines significantly (increased Snellen value) with decreases in luminance, at all contrast levels. However, the effect of contrast on NVG-aided VA is magnified at lower luminance levels, especially for contrast levels below 40% and image luminance values below 0.50 FL, indicating a non-linear relationship.

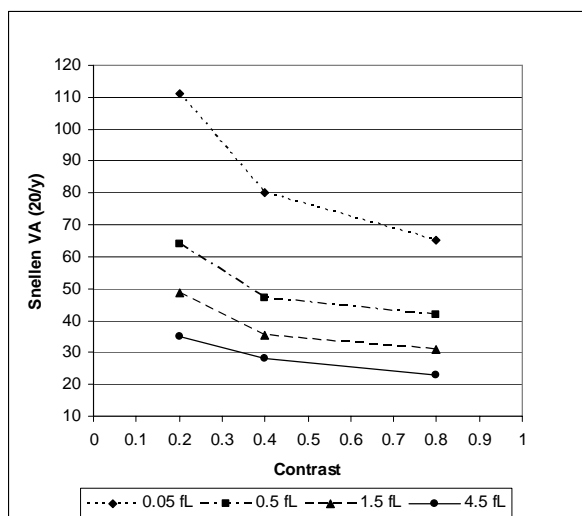


Fig. 10: NVG-aided visual acuity as a function of contrast and luminance

With conventional displays, the accuracy of NR_B , integrated luminance, and color balance oppose each other ultimately due to the fact that the NVG representation must over-emphasize red wavelengths in order to make up for the near infrared energy that is largely absent from the display output. Further complicating matters, if the red channel is to be the primary source of NVIS radiance available to the simulation, a single eight-bit modulation of NVG intensities is hardly enough to accommodate a large dynamic range in the scene. Traditionally, this is what forces NVG stimulation configurations into dim projector settings to mitigate the impact of low intensity precision. Small amounts of NVIS energy are present in the blue and green channels, but the relative levels of visible light make these channels of little use for NVG purposes. Given that the primary interest was in maximizing the precision and dynamic range of the NVG stimulation, spectral modulation approaches were investigated in an attempt to maximize the utility of the blue and/or green channels. It was found that aggressively filtering energy in the blue and green wavelengths in the blue and/or green projector guns can be an attractive method for gaining usable NR_B intensities allowing for more aggressive projector settings and dynamic range capability. This was due to the fact that the filtering technique brought the visible contribution of these guns from an unacceptably bright level back to a more natural level.

Ambient NR_B level is critical to the quality of the NVG stimulation regardless of projector configuration. Setting the goal for the ambient NR_B limit was derived by identifying minimum albedo to be accurately represented given the dimmest illumination scenario desired. 10% of starlight reflectance (approximately $4E-11 NR_B$) was found to be reliably achievable goal, although order 10^{-12} levels were often achievable.

Several observations were made with respect to the NVG optimization of various displays. For the most part, the display optimization approach depended upon the inherent dynamic range capabilities of the display. As an example, filtering of visible wavelengths tended to have more utility for brighter displays and less utility for inherently dimmer displays. This is largely due to the fact that 256 NVG intensities is an acceptable quantity if those intensities span a narrow enough dynamic range. Subjectively, this threshold seems to be very close to maximum reflective NR_B typical in a full moon scene. If a display system cannot produce NR_B output beyond this threshold, there is not anything to be gained by tapping the NR_B in the blue and green guns.

The two test cases capture the two extremes of dynamic range capability encountered in the study of CRT-based systems, and therefore provide a useful context for summarizing the approaches taken depending upon inherent dynamic range of a given system.

Test Case 1: Barco RetroGraphics with Filter Modifications

The Barco RetroGraphics system utilizes rear projection with a high gain (directional) projection surface of modest surface area. This combination results in high dynamic range. A three color progressive rendering technique was utilized exploiting the fact that all three guns would produce usable NR_B intensities. Fig. 11 summarizes the mapping of pixel value to NR_B inherent to the display and utilized in the render-

ing software. The radiance values for each pixel channel assume the sum of the contributions of any preceding color guns. Four NR_B reference values are marked in Fig. 11 to assist in judging scale. Lambertian values for CSL and FM correspond to typical NR_B levels measured off of a 100% diffuse reflector under clear starlight and full moon illumination conditions, respectively. The markers labeled “H60 Red” correspond to the at-sensor NR_B created by an H-60 external red position lamp at the viewing distances indicated. For unaided luminance correction, a gel filter was used on the blue and/or green projector lenses depending on simulated illumination condition. The spectral transmission of the filter used is found in Fig. 12.

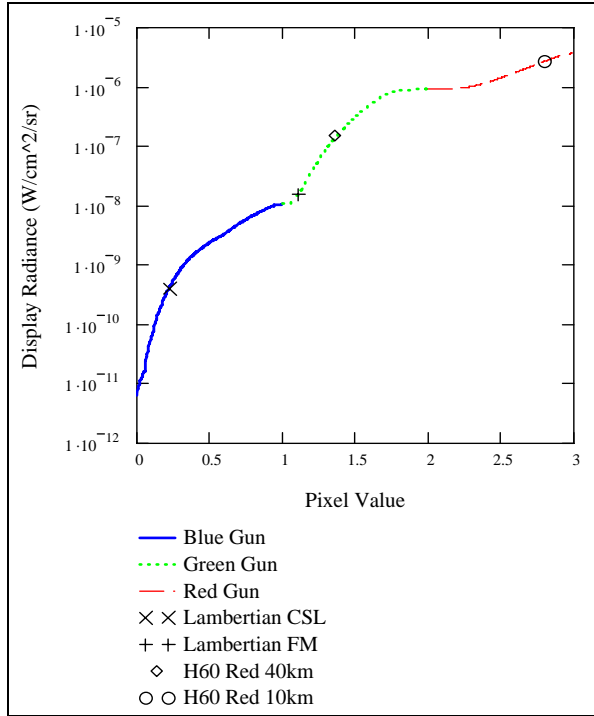


Fig. 11: Three color pixel-to-NRB mapping

The dynamic range data found in Table 5 summarizes the display in an unfiltered configuration. The luminance and radiance values in the numerical analysis that follows are associated with the display as filtered in the application.

Table 5: Barco RetroGraphics 801s characterization

CRT	Min (FL)	Max (FL)	Min (W/sr/cm ²)	Max (W/sr/cm ²)
Red	0	20	6.00E-12	2.72E-06
Green	0	47.3	6.00E-12	9.75E-07
Blue	2.50E-04	8.77	7.00E-12	1.04E-08

The test patches summarized in Table 6 were illuminated by simulated full-moon lunar illumination of 0.0345 foot-candles at terrain altitude (producing a luminance of 0.0345 foot-Lamberts (FL) on a simulated 100% lambertian surface). Similarly, the simulated lunar NR_B was 1.23E-8 W/cm²/sr. Under simulated starlight, the simulated NR_B produced on a 100% lambertian surface was 3.4E-10 W/cm²/sr. Unaided luminance levels were not evaluated as they were beyond the precision of the instruments used in the study.

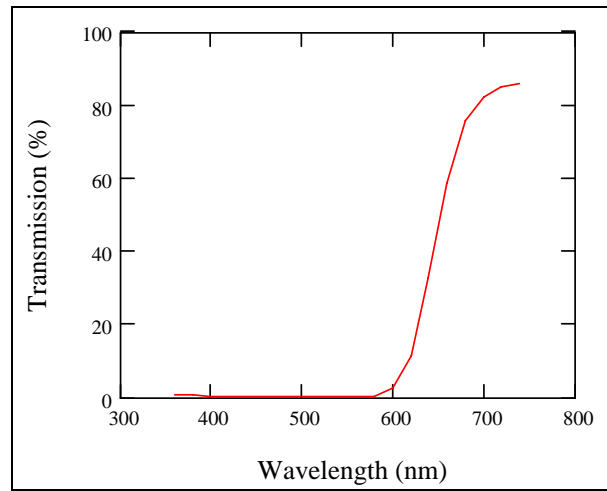


Fig. 12: Rosco #27 MED RED spectral transmission

Table 6: OTW luminance and NVG NR_B error

Lambertian Test Patch	Illumination	OTW Lum	NVG Lum	NR_B
		Intended Actual	Intended Actual	Intended Actual
10%	CSL	N/A	0.019	3.40E-11
		N/A	0.028	3.91E-11
100% disc	100% disc	0.003	2.197	1.23E-09
		0.000	2.147	1.21E-09
15%	CSL	N/A	0.062	5.81E-11
		N/A	0.062	5.81E-11
100% disc	100% disc	0.005	3.317	1.85E-09
		0.001	3.287	1.83E-09
25%	CSL	N/A	0.112	8.50E-11
		N/A	0.123	9.15E-11
100% disc	100% disc	0.009	4.108	3.09E-09
		0.001	4.104	3.05E-09
90%	CSL	N/A	0.513	3.06E-10
		N/A	0.587	3.47E-10
100% disc	100% disc	0.031	4.240	1.11E-08
		0.007	4.240	1.10E-08

The intended average scene luminance values found in Table 3 were derived by assuming a scene average of 25% of lunar sky radiance and 90% of starlight sky radiance.

Table 7: Average scene luminance (intended vs. actual)

Illumination	OTW Lum	NVG Lum
	Intended Actual	Intended Actual
CSL	N/A	0.513
	N/A	0.587
100% disc	0.009	4.108
	0.001	4.104

The intended and actual contrast values in Table 8 are derived from the luminance values found in Table 6.

Table 8: Contrast (intended vs. actual)

		Low Contrast	Med Contrast	High Contrast
		Intended	Intended	Intended
		Actual	Actual	Actual
NVG	CSL	20.00%	42.86%	80.00%
		19.54%	40.08%	79.75%
	100% disc	20.00%	42.86%	80.00%
		20.66%	43.31%	80.24%
OTW	CSL	n/a	n/a	n/a
		n/a	n/a	n/a
	100% disc	20.00%	42.86%	80.00%
		27.44%	54.16%	90.60%

Finally, the data from Table 7 and Table 8 are used to produce the visual acuity approximations found in Table 9. The differences between intended and actual NVG luminance and contrast (Table 7 and Table 8) are marginal and not likely to result in any reliable differences in NVG-aided VA. The intended and actual NVG-aided VA estimates provided in Table 9 were derived from the curves in Fig. 10, (using luminance values of 0.50 FL and 4.0 FL for CSL and 100% disc, respectively).

Table 9: Visual acuity (intended vs. actual)

		Low Contrast	Med Contrast	High Contrast
		Intended	Intended	Intended
		Actual	Actual	Actual
NVG	CSL	20/64	20/47	20/42
		20/64	20/47	20/42
	100% disc	20/35	20/28	20/23
		20/35	20/28	20/23

Results from Test Case #1 indicate that this configuration provides enough NR_B dynamic range and intensity precision to very accurately represent high, medium, and low contrast reflective scene content in starlight and full moon conditions. Further, the configuration provided the dynamic range to represent a point source having at-sensor radiance on the order of 10^{-6} .

Test Case 2: SEOS Panorama without Filter Mods

The SEOS Panorama system offers significant NVG utility due to its infinity focus configuration. The light loss in this configuration, however, presents challenges due to limited dynamic range. The maximum NR_B output of the system did not significantly exceed full moon NR_B . It was noted that the system was not bright enough to produce lightpoints capable of creating differing halo cues in the NVG, even with aggressive projectors brightness and contrast settings. Unaided luminance values were generally lower than desired indicating that the filtering method used was more aggressive than was needed.

Table 10: SEOS panorama characterization

CRT	Min (FL)	Max (FL)	Min (W/sr/cm ²)	Max (W/sr/cm ²)
Red	3.0E-4	1.01	3.2E-11	1.71E-7
Green	3.0E-4	1.31	3.3E-11	3.06E-8
Blue	3.0E-4	0.37	3.1E-11	5.51E-10

The system was first characterized and tested with a rendering and filtering approach like that utilized in Test Case #1. The results were similar to those achieved in Test Case #1 but with less than one-tenth of the NVG dynamic range. A simplified, red terrain only, radiance mapping was also implemented without filtering. Fig. 13 below shows the pixel mapping utilized for scene rendering in this configuration. In this case, the dynamic range performance was unchanged and the intensity precision was only modestly decreased, but the unaided representation was meaningfully brighter than natural levels. This configuration had the disadvantage of producing unaided terrain scenes that were completely red. Red was chosen due to the fact that it provides the most NR_B per quantity of unaided luminance. The use of any other projector gun would only make the unaided luminance even less accurate. While three-color rendering with filtering provided a more favorable color balance, it did not meaningfully improve the NR_B performance of the system due to the inherent dimness of the projection geometry. The numerical analysis below captures the single color, non-filtered configuration providing a quantification of the impact of the errors in the unaided scene.

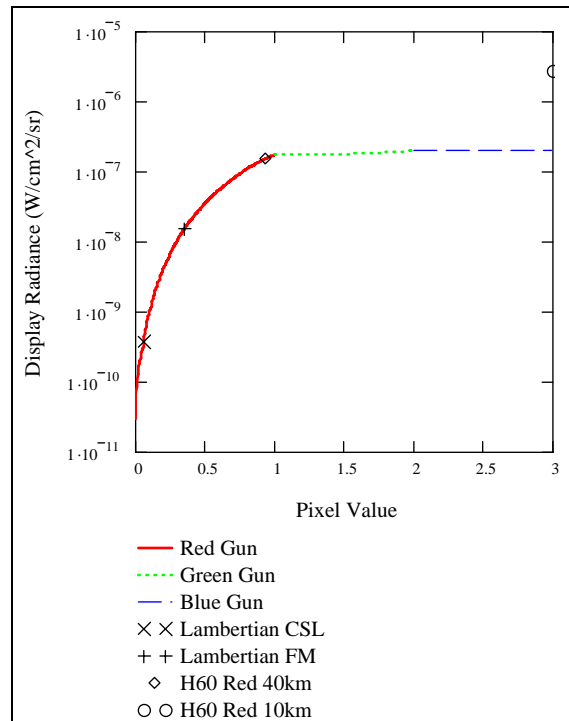


Fig. 13: Three color pixel-to- NR_B mapping

The test patches summarized in Table 11 were illuminated by simulated full-moon lunar illumination of 0.0345 foot-candles at terrain altitude (producing a luminance of 0.0345 FL on a simulated 100% Lambertian surface). Similarly, the simulated lunar NR_B was $1.23E-8$ W/cm²/sr. Under simulated starlight, the simulated NR_B produced on a 100% Lambertian was $3.4E-10$ W/cm²/sr. Unaided luminance levels

were not evaluated as they were beyond the precision of the instruments used in the study.

Table 11 OTW and NVG luminance error

Lambertian Test Patch	Illumination	OTW Lum	NVG Lum	NR _B
		Intended Actual	Intended Actual	Intended Actual
10%	CSL	N/A	0.019	3.40E-11
		N/A	0.012	3.00E-11
	100% disc	0.003	2.197	1.23E-09
		0.007	2.113	1.19E-09
15%	CSL	N/A	0.047	4.90E-11
		N/A	0.047	4.90E-11
	100% disc	0.005	3.317	1.85E-09
		0.010	3.136	1.75E-09
25%	CSL	N/A	0.112	8.50E-11
		N/A	0.116	8.72E-11
	100% disc	0.009	4.108	3.09E-09
		0.018	4.105	3.06E-09
90%	CSL	N/A	0.513	3.06E-10
		N/A	0.531	3.16E-10
	100% disc	0.031	4.240	1.11E-08
		0.065	4.240	1.09E-08

The intended average scene luminance values found in Table 12 were derived by assuming a scene average of 25% of lunar sky radiance and 90% of starlight sky radiance.

Table 12: Average scene luminance (intended vs. actual)

Illumination	OTW Lum	NVG Lum
	Intended Actual	Intended Actual
CSL	N/A	0.513
	N/A	0.531
100% disc	0.009	4.108
	0.018	4.105

Table 13: Contrast (intended vs. actual)

		Low Contrast	Med Contrast	High Contrast
		Intended Actual	Intended Actual	Intended Actual
NVG	CSL	20.00%	42.86%	80.00%
		24.15%	48.85%	82.69%
	100% disc	20.00%	42.86%	80.00%
		19.16%	44.03%	80.36%
OTW	CSL	n/a	n/a	n/a
		n/a	n/a	n/a
	100% disc	20.00%	42.86%	80.00%
		18.34%	44.58%	80.81%

The intended and actual contrast values in Table 13 are derived from the luminance values found in Table 11.

Finally, the data from Fig. 10, Table 12, and Table 13 are used to produce the visual acuity approximations found in Table 14 (using luminance values of 0.50 FL and 4.0 FL for CSL and 100% disc, respectively). As in Test Case #1, the differences between intended and actual NVG luminance and contrast (Tables 12 & 13) are marginal and not likely to result in significant differences in NVG-aided VA. The only condition in which a measurable change in VA could be predicted was at CSL (0.50 FL) and actual contrast of 24.15% versus an intended contrast of 20.00%.

Table 14: Visual acuity (intended vs. actual)

		Low Contrast	Med Contrast	High Contrast
		Intended Actual	Intended Actual	Intended Actual
NVG	CSL	20/64	20/47	20/42
		20/60	20/47	20/42
	100% disc	20/35	20/28	20/23
		20/35	20/28	20/23

Results from the second test case indicate that an 8-bit modulation of the red CRT alone provides satisfactory NR_B dynamic range and intensity precision to accurately represent high, medium, and low contrast terrain content in starlight and full moon conditions. The measurable NVG-aided acuity difference at low contrast indicates that this configuration represents the dynamic range at which quantization negatively impacts the accuracy. Stretching 256 intensities beyond this configuration will therefore introduce greater errors, particularly at low light levels. It is expected that even this adjustment would not support overcast starlight illumination conditions accurately. Without filtering or other display modifications, this would be the maximum dynamic range achievable for projectors having the same spectral characteristics, assuming visual performance accuracy is desired. In this configuration, the system provided the ability to represent a point source having at-sensor radiance on the order of 10⁻⁷, less than one-tenth that possible in Test Case #1. Also noted, the unaided luminance was twice that intended at full moon illumination. Further, the terrain and sky radiance is represented in red only. It would be possible in this case to create pixel combinations that contain allocations of blue and/or green. These combinations could be computed to have equal NR_B accuracy, but the unaided luminance errors would increase significantly.

Future Work

It is reasonable to assume that similar physics-based rendering techniques could be applied in luminance space in addition to NR_B space, although the research did not include this step. In such a full-spectrum rendering system, errors in display levels could be selectively allocated to the aided and unaided scene according to specific application requirements. The development of rendering algorithms that model the full spectrum of display output, not solely NR_B, are the next logical step for this approach. Development of this capability is in progress at AFRL/HEA.

Assessment of the impact of the OTW (unaided) scene luminance and contrast differences on visual performance warrants a more sophisticated, task-specific approach than that afforded by a visual acuity task. It would be desirable to develop a research protocol to evaluate NVG stimulation systems with regard to their impact on critical visual performance tasks such as visual search, target detection thresholds, and aircraft orientation/navigation in both aided and unaided contexts.

Finally, the research results offer opportunities to improve upon advanced rendering techniques and to consider new display capabilities and interfacing. Advancements, such as those discussed below, could make these results more repeatable, improve upon the accuracy of visible representations, or improve the dynamic range of aided and unaided representations.

Display Control Concepts

In considering the implementation of advanced physics-based simulation displays, it is helpful to first consider how such displays might be controlled in application.

Advanced Input Electronics. Most any display intended for the visual simulation market would benefit from an advanced input and control capability that takes physics-based quantities into consideration. Consider the utility that would be added if simulation applications could easily encode, in the pixel stream itself, the quantities of light (i.e. red radiance versus a unitless quantity of red) intended for each pixel on the display. Such technology would enable simplified exploitation of display-embedded auto-calibration techniques and would make physics-based representations far more accessible to software developers. While the implications to sensor-in-the-loop applications might be obvious, widespread use of quantitative visible-spectrum applications (i.e. physics-based visible color correction and contrast, and so forth) is also overdue. Such technology would have to include the communication of application-specific dynamic range mappings in order to preserve bandwidth on the hardware video bus. These coefficients could be communicated over a serial communication channel between the image generator and the display or perhaps over an auxiliary data channel carried via digital video. Emerging low cost digital video control electronics put advancements of this nature within reach.

Hardware support for data abstraction such as this would simplify the additional interfacing challenges that must be addressed. For example, all current image generation and display applications are built on a three-channel infrastructure. While it is tempting to assume that additional display channels could be added, one might first consider approaches that would be compatible with existing display interfaces. Table 3 summarizes the weighting of visible and NVIS bands present in the night sky. Future work, therefore, might investigate the suitability of novel approaches for mapping four-band simulations into three display channels. Any successful three-channel rendering approach will rely on an understanding of correlations or relationships between two of the four bands found above. While the spectra found in the night sky radiation defines certain correlations, those correlations are only completely accurate for neutral reflectors in the simulated scene. A more complete analysis might also consider the selective reflectivity of commonly-occurring vegetation, soil, and construction material classes. Similar consideration should also be given to the spectral properties of common man-made illuminators including cultural and battlefield emitters. In summary, future work

might investigate approaches to quantify and exploit correlations enhancing the accuracy of three-band simulations in the visible and near infrared domain. Example approaches might include:

1) **Consolidation of Correlated Wavelengths.** For example, suppose that three component video control systems were mapped to imaging components such that they modulate **Blue Radiance, Green Radiance, and NR_B** (rather than R, G, and B). This approach assumes that red and near infrared wavelengths are likely to be correlated in typical scenes, thereby mitigating the error created by collapsing them in application. In this example, this assumption is merely based on the proximity of the consolidated wavelengths. Such an assumption could be tested by surveying an appropriate sample of real-world reflective materials and optical emitters to determine if such a correlation exists. Such a survey might also find that a different correlation actually exists.

2) **Consolidation of Non-NVIS Wavelengths.** This approach makes no predictions regarding the errors associated with consolidation of the control of any two color bands, but rather makes the assumption that color balance errors created in the non-NVIS wavelengths will be acceptable in application (i.e., inaccuracies due to the consolidation will only appear in the unaided scene). For example, suppose that three component video control systems were configured to modulate **Green plus Blue Radiance, Red Radiance, and NR_B** . In such a configuration, a constant ratio of Blue to Green output could be engineered based upon an analysis of natural color balance like that summarized in Table 3.

3) **Consolidation of Visible Wavelengths.** Any three "color" control scheme is going to suffer from limited intensity precision, assuming no increase from the 8-bit capability that is prevalent today. This limited intensity is particularly problematic for producing realistic NVG scenes. This approach would seek to provide a higher precision control scheme for use with systems capable of high dynamic range. For example, suppose that three component video control systems were configured to modulate only **Visible Radiance and NR_B** , but dedicate two channels to the modulation of NR_B levels. In such a configuration, a constant ratio of Blue, Green, and Red output could be engineered based upon an analysis of natural color balance like that summarized in Table 3. Pixel-to-luminance mappings in the display could be engineered based upon a quantification of the night sky environment as was summarized in the Background. It is expected that a modified, more eccentric, gamma relationship would provide better simultaneous coverage of reflective levels and point-source levels. The ability to force varying gamma relationships according to simulated illumination condition would considerably improve the accuracy of aided and unaided representations.

Of course, four-band control is most desirable, cost permitting. Given the advancements in affordable digital controls, it is likely that the display industry will have more flexibility in implementing higher-granularity color control than can be expected from graphics hardware chipsets. With this in mind, and given the desire for greater precision in NR_B control, it might be most appropriate to look to two-node rendering approaches to control four-band displays. The three-color, radiance-mapped, rendering approach developed in this research will have direct applicability to such display technology concepts.

Display Implementation Concepts

The following display design concepts are offered as discussion of potential future research and development:

1) **Reconfigurable Embedded Spectral Filtering.** Support for turnkey filtering as described in the test cases, perhaps with multiple filtering options available per projectors gun, could provide a more repeatable capability with performance similar to that achieved in the study. Going a step further, the spectral transmission of the filter could be refined to better approximate the natural color balance of the night sky using the numerical analysis in the previous section. The filter used in the research transmitted approximately 0.03% and .05% of the blue and green energy, respectively. At those transmission levels, filtered luminance values were meaningfully lower than natural levels. A more optimized filtering specification could be produced according to a given projector's spectral characteristics. These enhancements alone would provide a high precision NVG stimulation mode for use when projection geometries allow for high dynamic range performance. Such a system would also be able to accurately match total integrated unaided luminance for the OTW scene (accommodating requirements for realistic OTW visual performance). Such enhancements, though, would rely on image generators with an inherent physics-based (or otherwise deterministic) rendering capability. The primary tradeoff to be concerned with in this configuration is the loss, in some measure, of the unaided representation of bright visible emitters (i.e. lightpoints) in the filtered color bands. Less aggressive filtering techniques will mitigate this tradeoff. Multiple filtering states would also allow the technique to be applied in varying projection geometries.

2) **Additional Integrated Conventional Projection Channel.** While it is more intuitive to consider adding a near infrared projection channel to conventional systems, the added expense of producing specialized components in small quantity has prevented these products from gaining significant traction in the industry. Also consider that a typical infra-red projector might produce little more, or possibly less, integrated NVIS radiance than a conventional red gun. In these cases, such a projector is only increasing the dynamic range capability of the integrated system by 2X, not a significant number compared to the dynamic range of the night environment (of which all projectors fall well short). Such a configuration might not exceed the NR_B performance produced by Test Case #1 described here. The goal of NR_B dynamic range and intensity precision consistent with Test Case #1 without sacrificing unaided luminance accuracy may be achievable by adding one or two additional, unfiltered, *conventional* projection channels to be utilized as luminance-correction channels. In this configuration an additional blue and/or green projection channel would be used to offset unaided luminance errors created by the filtering of other blue and/or green channel(s). Current research at AFRL/HEA is testing the viability of this concept by combining multiple projectors per visual channel. Availability of a turnkey system that mitigates the challenges of alignment and other adjustments would make the concept more viable.

3) **Enhance Near Infrared response in 3-CRT displays.** While not having the accuracy benefits of four separate display channels, the need for filtering (and the dynamic range impacts of not filtering) would be reduced if near infrared output of conventional displays were augmented to approximate the natural ratios present in night sky radiation. Phosphor sourcing and/or development would be aided by numerical analyses such as that summarized in Table 3 and by exploring the viability of three-channel control schemes as discussed

previously in this section.

4) **Separate IR projector.** Several IR projector products have been introduced, but current research did not include the characterization of any of such systems. In context of the current results, however, one can speculate with respect to those characteristics which might improve upon the performance now known to be achievable with techniques explored in the research. One could expect that a system producing energy in the near infrared wavelengths in larger quantities than in the visible wavelengths would provide some capacity to reduce the color balance and luminance errors associated with traditional systems. This capability alone, though, might not meet the expectations for such a system. To add substantial value, it would be desirable for specialized NVG displays to meaningfully address the limited dynamic capabilities of current systems. For example, suppose an IR CRT projector produced the same radiated power in the in the 700-1000 nm domain as traditional red CRT projectors produce in the 500-700 nm domain (i.e., when used in a projection geometry as in Test Case #1, suppose the IR projector produced order 10^{-7} NR_B). In this case, the NR_B dynamic range capability added by the addition of such a projector would perhaps be a 2x improvement. When attempting to produce a greater range of bright point sources, a 2x improvement is of little value. It would be meaningful to *add orders of magnitude* to the NR_B dynamic range. However, if the dynamic range were significantly larger than that of traditional systems, the typical 8-bit control electronics would be less than adequate. Therefore, higher precision control would have to be addressed in order to support a meaningful enhancement of dynamic range. The integration of traditional three-channel control electronics might provide an approach for higher precision control using false-color radiance rendering technique similar to that used in the current research.

5) **Additional Integrated Infrared Channel.** Integration of the IR channel with the visible channels would yield integration benefits including, ease of convergence and coordinated control as discussed previously. The challenges associated with the need for significant power and additional control bandwidth might make such a device particularly costly. The same physical advantages might also be achievable by implementing a remote coordination of the control and adjustment mechanisms.

Conclusions

The present research established that NR_B light levels can be produced for sensor-in-the-loop simulation in an accurate and predictable fashion by taking a physics-based approach to scene simulation and display integration.

In addition, this research defined and implemented an analytic approach for quantifying the inaccuracies in display NR_B output levels. Further, the impact to human visual acuity, as a result of NVG stimulation inaccuracies, was approximated. The results showed that quantitative, physics-based stimulation of NVGs can produce predictable, low-error results and that the unaided representation can be improved by selectively filtering visible wavelengths. Numerical analysis provided a foundation upon which more accurate filtering specifications can be developed.

References

- Berk, A., et al. (1989). MODTRAN: A Moderate Resolution Model for LOWTRAN 7. Air Force Geophysics Laboratory Technical Report GL-TR-89-0122, Hanscom AFB, MA.
- Biberman, L.M. (2000). Electro-Optical Imaging: System Performance and Modeling, Washington: SPIE Publications, pp. 3-1 – 3-14.
- Jensen, H. W., et al. (2001). A Physically-Based Night Sky Model. ACM SIGGRAPH 2001, 12-17 August 2001 (pp. 399-408). Los Angeles, CA: ACM SIGGRAPH.
- Lawrence, S.J., et al. (2003). A New Measurement of the Absolute Spectral Reflectance of the Moon. 34th Lunar and Planetary Science Conference, Abstract 1269 (p. 2) Lunar and Planetary Institute, Houston, TX.
- Leinert, Ch., et al. (1998). The 1997 Reference of Diffuse Night Sky Brightness. Astronomy, Astrophysics Supplement Series. 127, pp 1-99.
- Martin, L., et al. (2000). Physics Based Simulation of Night Vision Goggles, Proceedings of the Image Society. Scottsdale, AZ: The IMAGE Society.
- Moon, P. (1940). Proposed Standard Solar-Radiation Curves for Engineering Use. Journal of the Franklin Institute, 230 (5), pp. 583-617. Philadelphia, PA: Franklin Institute

Acknowledgements

This research and development was directed and co-sponsored by AFRL/HEA, Warfighter Readiness Research Division, Mesa, AZ, and Program Manager, Naval Air Training Systems, NAVAIR PMA205, NAS Patuxent River, MD, under contract F41624-97-D-5000.